DETERMINATION OF DISSOLUTION OF A MATERIAL WITH A MODERATELY-RAPID DISSOLUTION RATE

Thanutchaphorn Phupongskorn

A Thesis Submitted in Partial Fulfilment of the Requirements
for the Degree of Master of Science
The Petroleum and Petrochemical College, Chulalongkorn University
in Academic Partnership with
The University of Michigan, The University of Oklahoma,
Case Western Reserve University, and Institut Français du Pétrole
2012

Thesis Title:	Determination of Dissolution of a Material with a Moderately-rapid Dissolution Rate
By:	Thanutchaphorn Phupongskorn
Program:	Petrochemical Technology
Thesis Advisors:	Assoc. Prof. Thirasak Rirksomboon
	Prof. Derek H. Lister
	Prof. Frank R. Steward

Accepted by The Petroleum and Petrochemical College, Chulalongkorn University, in partial fulfilment of the requirements for the Degree of Master of Science.

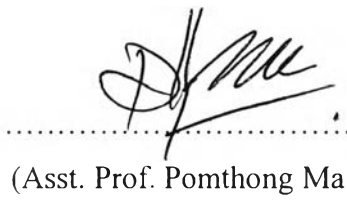

.....College Dean

(Asst. Prof. Pomthong Malakul)

Thesis Committee:

(Assoc. Prof. Thirasak Rirksomboon)

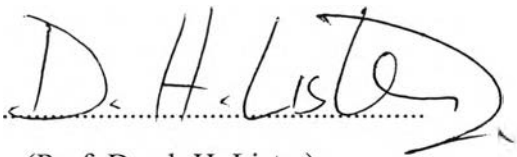

(Prof. Derek H. Lister)

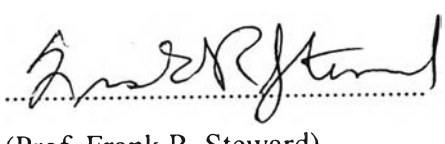

(Prof. Frank R. Steward)

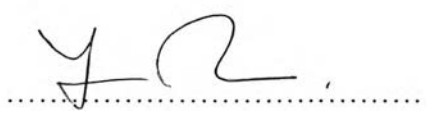

(Dr. Boonrod Sajjakulnukit)

(Prof. Anuvat Sirivat)

ABSTRACT

5371027063: Petrochemical Technology Program
Thanutchaphorn Phupongskorn: Determination of Dissolution of a Material with a Moderately-rapid Dissolution Rate
Thesis Advisors: Assoc. Prof. Thirasak Rirksomboon, Prof. Derek H. Lister, and Prof. Frank R. Steward, 122 pp.

Keywords: Jet-impingement/ Dissolution/ Mass-transfer

In common industrial process, mass transfer control and dissolution control (mixed control) or dissolution control can be involved for designing process equipment or determining the mechanisms of chemical reactions. A jet-impingement apparatus has been used to study dissolution rates by directing a jet of water onto a pellet of the material of interest at high velocity to ensure that dissolution is controlling. The apparatus has been used to measure the dissolution rate constant of magnetite under the conditions of power system coolants – often a controlling parameter in steel corrosion. For unequivocal measurements of the dissolution rate constant, the mass transfer characteristics of the apparatus need to be known in order to extrapolate mass transfer coefficients to the conditions of interest. Accordingly, mass transfer in our impingement system is being studied at atmospheric pressure with materials of a moderate dissolution rate. Cast pellets of plaster of Paris of different purities and single crystals of the same compound (gypsum – $CaSO_4 \cdot 2H_2O$), and pellets of trans-cinnamic acid, potassium bitartrate and aspartic acid have been used in this study. The dissolution rate constants for single crystal and aspartic acid were determined and the commercial plaster result gave mass-transfer correlation of jet-impinging apparatus in reasonable agreement with published correlation. However, the commercial plaster tended to have a higher solubility than pure plaster or gypsum crystals; its dissolution rates were higher than those of the other materials studied, which were in the same range.

บทคัดย่อ

ธนัชพร ภู่พงศกร : ชื่อหัวข้อวิทยานิพนธ์ การศึกษาการสลายตัวของวัสดุ ด้วยอัตราการสลายตัวอย่างรวดเร็ว (Determination of Dissolution of a Material with a Moderately-rapid Dissolution Rate) อ.ที่ปรึกษา : รศ. ดร. ธีรศักดิ์ ฤกษ์สมบูรณ์ ศ. ดร. ดีเรก เอช ลิสเตอร์ และ ศ. ดร. แฟรงค์ อาร์ สจ๊วต 122 หน้า

การควบคุมโดยการถ่ายเทมวลสาร การควบคุมทั้งการถ่ายเทมวลสาร และการสลายตัวของวัตถุ หรือ การควบคุมโดยการสลายตัวของวัตถุเพียงอย่างเดียว มีความเกี่ยวข้องในอุตสาหกรรมการผลิตทั่วไปสำหรับการออกแบบกระบวนการผลิตและการทำนายกระบวนการทางปฏิกริยาเคมี ระบบการไหลแบบพุ่งชน (Jet- impinging) ใช้ในการศึกษาอัตราการสลายตัวโดยการฉีดน้ำลงบนพื้นผิวเม็ดตัวอย่างของวัสดุที่สนใจด้วยความเร็วสูงเพื่อรับรองว่าระบบจะถูกควบคุมโดยการสลายตัวของวัสดุ ระบบการไหลแบบพุ่งชนเดียวกันนี้ได้ถูกใช้เพื่อวัดอัตราการสลายตัวของแมกนีไทต์ (Magnetite; Fe_3O_4) ภายใต้สภาวะของระบบหล่อเย็น ซึ่งแมกนีไทต์นี้เป็นหนึ่งในตัวแปรของการกัดกร่อนในเหล็ก สำหรับการวัดค่าคงที่ของการสลายตัวอย่างแม่นยำจำเป็นต้องทราบค่าถ่ายเทมวลสารของระบบเพื่อทำการจำลองสู่สภาวะที่สนใจ การถ่ายเทมวลสารของวัสดุในการทดลองนี้ได้ถูกศึกษาที่ความดันบรรยากาศด้วยอัตราการสลายตัวอย่างรวดเร็ว เม็ดตัวอย่างทรงกระบอกที่ทำจากยิปซัมจากการผสมปูนพลาสเตอร์ (Plaster of Paris) ที่ความบริสุทธิ์ต่างกัน ผลึกยิปซัม (Single crystal of gypsum) ที่มีส่วนประกอบเดียวกัน ($CaSO_4 \cdot 2H_2O$) กรดทรานซินนามิกส์ โพแทสเซียมไบทาเตรต และ กรดแอสพาติกได้ถูกนำมาศึกษาในงานวิจัยนี้ ค่าคงที่การสลายตัวของยิปซัมคริสตัลและกรดแอสพาติกสามารถหาได้จากการทดลองนี้ซึ่งใกล้เคียงกับงานวิจัยที่ถูกตีพิมพ์ ผลการทดลองของยิปซัมจากปูนพลาสเตอร์ที่ความบริสุทธิ์ทั่วไปให้สมการความสัมพันธ์ของระบบการไหลแบบพุ่งชนที่สอดคล้องกับสมการความสัมพันธ์ในงานวิจัยที่ถูกที่ตีพิมพ์ อย่างไรก็ตามค่าความสามารถในการละลายของยิปซัมจากปูนพลาสเตอร์ที่ความบริสุทธิ์ทั่วไปมีแนวโน้มจะสูงกว่ายิปซัมจากปูน พลาสเตอร์ที่ความบริสุทธิ์สูง และ ผลึกยิปซัม เนื่องจากค่าอัตราการสลายตัวสูงกว่าวัสดุอื่นซึ่งอยู่ในช่วงเดียวกัน

ACKNOWLEDGEMENTS

I am grateful for the scholarship and funding of the thesis work provided by the Petroleum and Petrochemical College; and the Center of Excellence on Petrochemical and Materials Technology, Thailand.

My research work would not be completed well without the assistance and support of people who have cooperated in this research.

First of all, I would like to thank my advisors, Prof. Derek H. Lister, Prof. Frank R. Steward and Assoc. Prof. Thirasak Risksomboon for giving me an opportunity to carry out my research at the University of New Brunswick, Canada.

My research work cannot be completed without the valuable guidance, the intensive support, patience and endless help throughout this research work of Prof. Derek H. Lister. I am very appreciative of all his advice and it is my honor to have him as my supervisor.

Next, I would like to extend my special thanks to staffs and students of UNB Nuclear group which are Dr. Lihui Liu, Dr. Noel Kippers, Dr. Thananchai Piroonpan, Dr. Kittima Khumsa-Ang, Mr. Piti Srisukvatananan, Miss Pimsiri Phromwong, Miss Khatereh Mohajery for good advice and technical support though this research work.

Further, I would like to thanks Mr.Steven Cogswell, Mr. Keith Rollins, and Mr. Adon Briggs for helping me analyse my samples, and giving me technical supports and useful information and suggestion.

Moreover, I would like to give a special thanks to Prof. Frank R. Steward and his wife who have helped me and taken care of me during my stay in Canada and to all Thai community and Thai student associate (THASA) for their friendship, standing beside me and cheering me up. I will keep these precious memories with me forever.

Finally, I would like to give my deepest gratitude to my beloved family in Thailand for their support, unconditional love, blessing, encouragement and cheering me up.

TABLE OF CONTENTS

		PAGE
Title Page		i
Abstract (in English)		iii
Abstract (in Thai)		iv
Acknowledgements		v
Table of Contents		vi
List of Tables		xi
List of Figures		xiv
Abbreviations		xx
List of Symbols		xxi
CHAPTER		
I	**INTRODUCTION**	1
II	**LITERATURE REVIEW**	3
	2.1 Principles of Corrosion of Materials	3
	2.1.1 Definition of Corrosion	3
	2.1.2 Types of Corrosion	4
	2.2 Physical Methods Investigation	5
	2.2.1 Fundamental Principles of Scanning Electron Microscopy (SEM)	5
	2.2.2 Fundamental Principles of Dial Indicator	6
	2.3 Flow-Accelerated Corrosion (FAC)	7
	2.4 Oxide Film	9
	2.5 Scalloped Surface	13
	2.6 Plaster of Paris ($CaSO_4 \cdot 1/2H_2O$)	14
	2.7 Gypsum Crystal Characteristics	15
	2.8 Dissolution Rate of Crystal of Gypsum and Plaster of Paris	16

CHAPTER PAGE

2.8.1 The Effect of Temperature on Dissolution of Crystal of Gypsum and Plaster of Paris Pipe 20
2.8.2 Pressure Drop 21
2.8.3 The Effect of pH 23
2.8.4 The Surface behavior of Crystal of Gypsum During Dissolution 26
2.9 Trans-Cinnamic Acid Characteristics 26
2.10 Potassium Bitartrate Characteristics 27
2.11 L-Aspartic Acid Characteristics 28
2.11.1 Dissolution of L-aspartic Acid 29
2.12 Jet Impingement Study 30
2.12.1 Hydrodynamic Characteristics 30
2.12.2 Mass Transfer 31

III EXPERIMENTAL 35
3.1 Materials and Equipment 35
3.1.1 Equipment 35
3.1.2 Instrument 35
3.1.3 Chemicals 36
3.2 Experimental Procedures 36
3.2.1 Gypsum Pellet Preparation 37
3.2.1.1 Plaster of Paris ($CaSO_4 \cdot 1/2H_2O$) 37
3.2.1.2 Single Crystal of Gypsum 38
3.2.1.3 Trans-Cinnamic acid 38
3.2.1.4 Potassium Bitartrate 38
3.2.1.5 Aspartic Acid Powder 38
3.3 Test Loop 39
3.4 Test Section 40
3.5 Test Conditions 41

CHAPTER **PAGE**

3.5.1 Plaster of Paris ($CaSO_4 \cdot 1/2H_2O$) 41

3.5.1.1 Commercial Plaster of Paris 41

3.5.1.2 Pure Plaster of Paris 42

3.5.2 Single Crystal of Gypsum 43

3.5.3 Trans-Cinnamic Acid and Potassium Bitartrate 43

3.5.4 L-Aspartic acid 44

3.6 Analytical Techniques 44

3.6.1 Characterization of Pellet Surface 44

3.6.2 Dissolution Rate and Mass Transfer of Pellet 44

IV RESULTS AND DISCUSSION 47

4.1 Commercial Plaster of Paris 47

4.1.1 Pellet Surface Characteristics 47

4.1.2 Weight Loss 49

4.1.3 Dissolution Rate 51

4.1.4 Overall Rate Constant 53

4.2 Pure Plaster of Paris 55

4.2.1 Pellet Surface Characteristics 55

4.2.2 Weight Loss 58

4.2.3 Dissolution Rate 59

4.2.4 Overall Rate Constant 61

4.3 Potassium Bitartrate 63

4.3.1 Pellet Surface Characteristics 63

4.3.2 Weight Loss 65

4.3.3 Dissolution Rate 66

4.3.4 Overall Rate Constant 67

4.4 L-Aspartic Acid 69

4.4.1 Pellet Surface Characteristics 69

4.4.2 Weight Loss 72

CHAPTER		PAGE
	4.4.3 Dissolution Rate	73
	4.4.4 Overall Rate Constant	74
	4.5 Trans-Cinnamic Acid	76
	4.5.1 Pellet Surface Characteristics	76
	4.5.2 Weight Loss	77
	4.5.3 Dissolution Rate	78
	4.5.4 Overall Rate Constant	79
	4.6 Single Crystal	80
	4.6.1 Pellet Surface Characteristics	80
	4.6.2 Weight Loss	82
	4.6.3 Dissolution Rate	82
	4.6.4 Overall Rate Constant	83
	4.7 Materials comparison	84
	4.7.1 Pellet Surface Characteristics	84
	4.7.2 Weight Loss	87
	4.7.3 Dissolution Rate	88
	4.7.4 Overall Rate Constant	89
	4.8 Apparatus Correlations	90
V	**CONCLUSIONS AND RECOMMENDATIONS**	94
	REFERENCES	95
	APPENDICES	102
	Appendix A Pellet Profiles	102
	Appendix B Thermophysical Properties of Water	117
	Appendix C Diffusion at Infinite Dilution	118
	Appendix D Transformations of the Coordinates	121

PAGE

CURRICULUM VITAE 122

LIST OF TABLES

TABLE		PAGE
2.1	Types of Corrosion (Grundke,1976)	4
2.2	Physico-Chemical Characteristics of gypsum. (Amethyst Galleries, Inc., 2011, Wallace A. G., 2003 and Gypsum in Handbook of Mineralogy, 2005)	16
2.3	Physico-Chemical Characteristics of trans-cinnamic acid. (Acros Organics BVBA Inc., 2012, Delgado J. M. P. Q., 2007)	27
2.4	Physico-Chemical Characteristics of potassium bitartrate. (Fisher Scientific Company, 2012)	28
2.5	Physico-chemical characteristics of l-aspartic acid. (Fisher Scientific Company, 2012, Lin S., 2006)	29
2.6	The kinetic parameters determined from dissolution of monodisperse crystals of l-aspartic acid (k: cm min^{-1}) (Shan et al., 2001)	30
2.7	Summary of Sherwood number equations (Pierrefeu, D. L., 2009)	33
3.1	Runs for studying the effect of flow rates by using Plaster of Paris mixed with de-ionized water (pH 7 ± 1, pressure 1 atm, 3 mins, 25 ^{o}C)	42
3.2	Runs for studying the effect of flow rates by using pure plaster (pH 7 ± 1, pressure 1 atm, 10 mins)	43
3.3	Runs for studying the effect of flow rates by using single crystal (pH 7 ± 1, pressure 1 atm, 30 mins, 120 ml/min, 20 ^{o}C)	43
4.1	The effect of flow rate on volume lost and weight loss in commercial plaster of Paris	51

TABLE **PAGE**

4.2	Dissolution rate of commercial plaster of Paris with different flow rates	53
4.3	Overall rate constant of commercial plaster of Paris with different flow rates	55
4.4	The effect of flow rate on volume lost and weight loss in pure plaster of Paris	59
4.5	Dissolution rate of pure plaster of Paris with different flow rates	61
4.6	Overall rate constant of pure plaster of Paris with different flow rates	62
4.7	The effect of flow rate on volume lost and weight loss in potassium bitartrate	66
4.8	Dissolution rate of potassium bitartrate with different flow rates	67
4.9	Overall rate constant of potassium bitartrate with different flow rates	68
4.10	The effect of flow rate on volume lost and weight loss in L-aspartic acid	73
4.11	Dissolution rate of l-aspartic acid with different flow rates	74
4.12	Overall rate constant of l-aspartic acid with different flow rates	75
4.13	The effect of flow rate on volume lost and weight loss in trans-cinnamic acid	78
4.14	Dissolution rate of trans-cinnamic acid with different flow rates	79
4.15	Overall rate constant of trans-cinnamic acid with different flow rates	80

TABLE **PAGE**

4.16	The effect of pellet size on volume lost and weight loss in single crystal	82
4.17	Dissolution rate of single crystal with different size	83
4.18	Overall rate constant of single crystal with different size	83
4.19	Comparison of Sherwood number from different correlations	92
B1	Thermophysical Properties of Water (CRC Handbook, 2011)	117
C1	Diffusion at Infinite Dilution (CRC Handbook, 2011)	118

LIST OF FIGURES

FIGURE		PAGE
2.1	Dial inspector (Edward J. Bennett Company, 2005).	6
2.2	FAC risk zone (Koshizuka et al, 2010 and Naitoh et al, 2008).	8
2.3	Sketch of the growth mechanism of the Fe_3O_4 film (Zhu et al, 2006).	11
2.4	A schematic view of the formation mechanism of the magnetite film on the steel surface in high temperature water (Cheng and Steward, 2004).	12
2.5	Evolution of a surface according to (1) Passive–bed Theory and (2) Defect Theory (Villien et al, 2001).	14
2.6	Dihydrate solubility in H_2O vs. temperature. (Azimi et al.,2007)	19
2.7	Dissolution rate on plaster of Paris pipe with time at different temperatures, 0.21-0.25 mm, 50 defects/cm^3 and 25 LPM. (Warunphaisal, 2009).	21
2.8	The pressure drop versus time (Shao, 2006).	21
2.9	Pressure drop with time at pH 3, 30 °C (Warunphaisal, 2009).	23
2.10	Dependence of Ca^{+2} concentration on the OH^- concentration in the solution with and without sulfate (Rachenberg and Sprung, 1983).	24
2.11	Gypsum solubility in H_2SO_4 solutions at different temperatures (Azimi, 2007).	24
2.12	Comparison of dissolution rates at difference pHs (Sinthuphan, 2008).	25

FIGURE **PAGE**

2.13	Dissolution rate along a plaster of Paris pipe at 25 LPM, 30 °C (Warunphaisal, 2009).	25
2.14	Etch pits formed on gypsum (010)-A (A) and (010)-B (B) surfaces. Note that the morphologies of the pits in (A) and (B) are mirror images of each other (Fan and Teng, 2007).	26
2.15	Hydrodynamic characteristics of jet impingement on a flat plate showing the four characteristic flow regions (Efird et al., 1993).	31
3.1	Drawing of Teflon holder (in millimeter unit).	36
3.2	Schematic of the mixing apparatus (Villien et al., 2001).	37
3.3	Schematic of gypsum pellet.	38
3.4	Schematic of water loop for the dissolution rate experiment.	39
3.5	Schematic diagram of the test section.	41
4.1	Surface of commercial plaster of Paris pellet at different flow rates at 25 ^{o}C for 3 minutes.	47
4.2	Surface of commercial plaster of Paris pellet at different flow rates at 25 ^{o}C for 3 minutes.	48
4.3	Surface of commercial plaster of Paris pellet at different flow rates at 25 ^{o}C for 3 minutes.	49
4.4	The effect of flow rate on weight loss of commercial plaster of Paris pellet.	50
4.5	Dissolution rate of commercial plaster of Paris with different flow rates.	52
4.6	Overall rate constant of commercial plaster of Paris with different flow rates.	54
4.7	Surface of pure plaster of Paris pellet at different flow rates at 35^{o}C for 10 minutes.	56

FIGURE **PAGE**

4.8	Surface of pure of Paris pellet at different flow rates at 35 oC for 10 minutes.	57
4.9	Surface of pure of Paris pellet at different flow rates at 35°C for 10 minutes.	58
4.10	The effect of flow rate on weight loss of pure plaster of Paris pellet.	59
4.11	Dissolution rate of pure plaster of Paris with different flow rates.	60
4.12	Overall rate constant of pure plaster of Paris with different flow rates.	62
4.13	Surface of potassium bitartrate pellet at different flow rates at 20 °C for 10 minutes.	63
4.14	Surface of potassium bitartrate pellet at different flow rates at 20°C for 10 minutes.	64
4.15	Surface of potassium bitartrate pellet at different flow rates at 20°C for 10 minutes.	65
4.16	The effect of flow rate on weight loss of potassium bitartrate pellet.	66
4.17	Dissolution rate of potassium bitartrate with different flow rates.	67
4.18	Overall rate constant of potassium bitartrate with different flow rates.	68
4.19	Surface of l-aspartic acid pellet at different flow rates at 20 °C for 5 minutes.	70
4.20	Surface of l-aspartic acid pellet at different flow rates at 20 °C for 5 minutes.	71
4.21	Surface of l-aspartic acid pellet at different flow rates at 20 °C for 5 minutes.	72

FIGURE **PAGE**

4.22	The effect of flow rate on weight loss of l-aspartic acid pellet.	73
4.23	Dissolution rate of l-aspartic acid with different flow rates.	74
4.24	Overall rate constant of l-aspartic acid with different flow rates.	75
4.25	Surface of trans-cinnamic acid pellet at different flow rates at 20 °C for 10 minutes.	76
4.26	Surface of trans-cinnamic acid pellet at different flow rates at 20 °C for 10 minutes.	77
4.27	The effect of flow rate on weight loss of trans-cinnamic acid pellet.	78
4.28	Dissolution rate of trans-cinnamic acid with different flow rates.	79
4.29	Overall rate constant of trans-cinnamic acid with different flow rates.	80
4.30	Surface of single crystals at different diameters exposed at 20 °C for 30 minutes.	81
4.31	Surfaces of pellets of different materials.	85
4.32	Surfaces of pellets of different materials.	86
4.33	Surfaces of pellets of different materials.	87
4.34	Weight losses of cast pellets of various materials.	88
4.35	Dissolution rates of cast pellets of various materials.	89
4.36	Overall rate constants of cast pellets of various materials.	90
4.37	Sherwood number plot for dissolution of cast pellets of various materials.	91
A.1	Commercial plaster profile at 40 ml/min and 25 °C.	102
A.2	Commercial plaster profile at 60 ml/min and 25 °C.	102
A.3	Commercial plaster profile at 80 ml/min and 25 °C.	103

FIGURE **PAGE**

A.4	Commercial plaster profile at 100 ml/min and 25 oC.	103
A.5	Commercial plaster profile at 120 ml/min and 25 oC.	103
A.6	Commercial plaster profile at 140 ml/min and 25 °C.	104
A.7	Commercial plaster profile at 160 ml/min and 25 °C.	104
A.8	Commercial plaster profile at 180 ml/min and 25 °C.	104
A.9	Commercial plaster profile at 199 ml/min and 25 °C.	105
A.10	Pure plaster profile at 40 ml/min and 35 °C.	105
A.11	Pure plaster profile at 60 ml/min and 35 °C.	105
A.12	Pure plaster profile at 80 ml/min and 35 °C.	106
A.13	Pure plaster profile at 100 ml/min and 35 °C.	106
A.14	Pure plaster profile at 120 ml/min and 35 °C.	106
A.15	Pure plaster profile at 140 ml/min and 35 °C.	107
A.16	Pure plaster profile at 160 ml/min and 35 °C.	107
A.17	Pure plaster profile at 180 ml/min and 35 °C.	107
A.18	Big single crystal profile at 120 ml/min and 20 °C.	108
A.19	Small single crystal profile at 120 ml/min and 20 °C.	108
A.20	Potassium bitatrate profile at 40 ml/min and 20 °C.	108
A.21	Potassium bitatrate profile at 60 ml/min and 20 °C.	109
A.22	Potassium bitatrate profile at 80 ml/min and 20 °C.	109
A.23	Potassium bitatrate profile at 100 ml/min and 20 °C.	109
A.24	Potassium bitatrate profile at 120 ml/min and 20 °C.	110
A.25	Potassium bitatrate profile at 140 ml/min and 20 °C.	110
A.26	Potassium bitatrate profile at 160 ml/min and 20 °C.	110
A.27	Potassium bitatrate profile at 180 ml/min and 20 °C.	111
A.28	Aspartic acid profile at 40 ml/min and 20 °C.	111
A.29	Aspartic acid profile at 60 ml/min and 20 °C.	111
A.30	Aspartic acid profile at 80 ml/min and 20 °C.	112
A.31	Aspartic acid profile at 100 ml/min and 20 °C.	112

FIGURE **PAGE**

A.32	Aspartic acid profile at 120 ml/min and 20 oC.	112
A.33	Aspartic acid profile at 140 ml/min and 20 oC.	113
A.34	Aspartic acid profile at 160 ml/min and 20 oC.	113
A.35	Aspartic acid profile at 180 ml/min and 20 °C.	113
A.36	Trans-cinnamic acid profile at 40 ml/min and 20 °C.	114
A.37	Trans-cinnamic acid profile at 60 ml/min and 20 °C.	114
A.38	Trans-cinnamic acid profile at 80 ml/min and 20 °C.	114
A.39	Trans-cinnamic acid profile at 100 ml/min and 20 °C.	115
A.40	Trans-cinnamic acid profile at 120 ml/min and 20 °C.	115
A.41	Trans-cinnamic acid profile at 140 ml/min and 20 °C.	115
A.42	Trans-cinnamic acid profile at 160 ml/min and 20 °C.	116
A.43	Trans-cinnamic acid profile at 180 ml/min and 20 °C.	116

ABBREVIATIONS

BSE	Backscattered electrons
CANDU	Canada deuterium uranium
CL	Cathodoluminescence
CSD	Crystal size distribution
DSC	Differential scanning calorimeter
EDX	Energy Dispersive X-ray Analysis
FAC	Flow-Accelerated Corrosion
LWR	Light Water Reactor
MSE	Mixed-solvent-electrolyte
PAL	Phenylalanine ammonia-lyase
SEM	Scanning electron microscope

LIST OF SYMBOLS

C_b	Bulk Concentration
C_p	Isobaric heat capacity (kJ/ kgK)
C_s	Concentration at the surface (solubility)
C_v	Isochoric heat capacity (kJ/ kgK)
D	Diffusion coefficient
D_{AW}	Diffusivity of species A in water (m^2/s)
D_p	Pipe diameter (m)
d_0	Nozzle diameter (m)
H	Enthalpy (kJ/kg)
K	Overall rate constant for dissolution, Dissolution coefficient (m/s)
k_d	Dissolution rate constant (m/s)
k_m	Mass transfer coefficient (m/s)
k_t	Mass transfer coefficient
L	Characteristic linear dimension (m)
$(L_1-L_2)_p$	Length of pipe (m)
m_{eq}	Molal equilibrium concentration
P	Pressure drop (Pa)
R	Overall dissolution rate
R_o	Ratio of water-to-powder
Re	Reynolds number
S	Entropy (kJ/kgK)
Sc	Schmidt number
Sh	Sherwood number
T	Temperature (°C)
u	Speed of sound (m/s)
v	Flow velocity (m/s)
x	Position of Interested

y	Depth at position of interest (m)
ρ	Fluid density (kg/m^3)
δ	Diffusion layer thickness
Ω	C_b/ C_s
ζ	Transport reaction factor
μ	Dynamic viscosity of the fluid ($Pa \cdot s$ or $N \cdot s/m^2$ or $kg/(m \cdot s)$
ν	Kinematic viscosity (m^2/s)
H	Viscosity (μPas)
Λ	Thermal conductivity (mW/mK)